CRYSTAL STRUCTURES OF INTERMETALLICS AND PHASE EQUILIBRIA IN THE Pd-Lu SYSTEM

N.B. Kolchugina

BAIKOV INSTITUTE OF METALLURGY AND MATERIALS SCIENCE, Leninskii pr. 49, Moscow, 119991 Russia, natalik@imet.ac.ru

Abstract

X-ray diffraction analysis, DTA, and electron microscopy were used to study the crystal structures and formation sequence of intermetallics in the Lu-Pd system for compositions Pd-(0-50 at. %) Lu. The alloys were synthesized using high-purity Lu. The system is characterized by terminal Pd-based solid solutions up to 10 at.% Lu (at 1000°C) and a number of intermetallics (Lu_3Pd_4, Lu_2Pd_3, LuPd, $LuPd_3$, $Lu_{10}Pd_{21}$). A nonequilibrium bertholide phase was found is formed in a composition range of from 40 to 50 at. % Lu. The phase diagram in a composition range of Pd-(0-50 at. %) Lu is given.

1. INTRODUCTION

Phase diagrams of palladium with different rare-earth metals are similar; compounds, which are formed in the systems and have similar stoichiometries, are isotypic [1]. The phase diagrams of the majority of the palladium – rare-earth metal REM (REM = Sm, Gd, Ho, Dy, Tb, Tb, Y) systems are available [2]. The systems in a range of REM concentrations of 0-50 at. % are characterized by a terminate Pd-based solid solution and five intermetallic compounds; these are $REMPd_3$, $REM_{10}Pd_{21}$, REM_2Pd_3, REM_3Pd_4, and REMPd [3]. Up to now, no complete phase diagram of the Pd-Lu system is available. The Pd-Lu system in a range of 0-25 at. % Lu was studied in [4] and the portion of the phase diagram is presented, which was constructed using differential thermal analysis (DTA) and X-ray diffraction (XRD) data. The presence of $LuPd_3$- and Pd-based solid solutions was shown. The Pd-based solid solutions with REMs exhibit anomalously high hydrogen permeability [5]. Moreover, compounds of the Pd-REM systems were found to exhibit unique optical properties. The most pronounced optical properties were found just for $LuPd_3$ and LuPd compounds, which are blue (similar to silicon) and golden, respectively [6].

The aim of the present study is to determine the phase equilibria in the Lu-Pd system in a range of compositions of from 25 to 50 at. % Lu and to construct the portion of the Pd-Lu phase diagram for a composition range of 0-50 at. % Lu.

2. EXPERIMENTAL

The Lu-Pd alloys with 30, 35, 44.5, and 45.7 at. % Lu and compositions corresponding to stoichimetric compounds $Lu_{10}Pd_{21}$, Lu_2Pd_3, and Lu_3Pd_4, were prepared by arc melting in a purified argon atmosphere using a nonconsumable tungsten electrode and a copper water-cooled bottom. To ensure composition homogeneity of the ingots, we melt them repeatedly and annealed for homogenization. We used PDA-1 palladium and high-purity lutetium, which preliminarily was purified by vacuum distillation. The purification is performed at a residual pressure of 10^{-4}-10^{-5} Pa in a resistor furnace equipped with a graphite heater. A purified metal is evaporated from a tantalum crucible and deposited

on a water-cooled copper condenser in the form of a druse of small crystals growing together. The spacing between the condenser and molten metal is equal to 40-45 mm; the spacing can be varied with graphite tables. The melting chamber is evacuated with roughing-down and diffusion pumps. Molybdenum cylindrical shields are placed between the graphite heater and furnace walls. The impurity compositions of initial (commercial) and purified lutetium were studied by laser mass spectrometry. Figure 1 demonstrates changes in the impurity composition of lutetium after vacuum distillation.

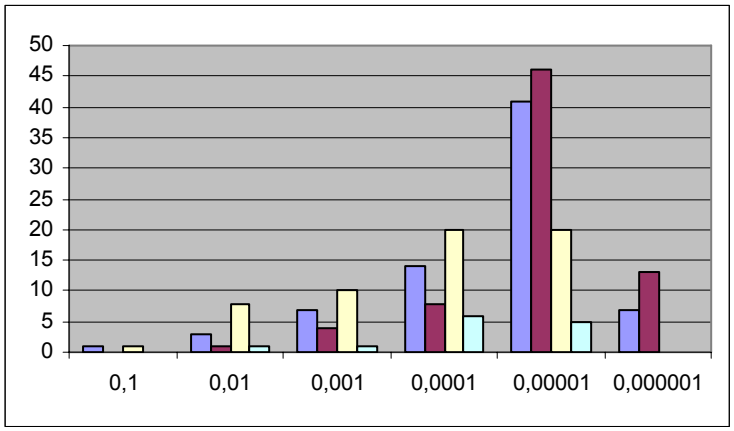

Fig. 1. Changes in the impurity distribution in lutetium after vacuum distillation. Blue, red, and white columns correspond to number of impurities (whose contents correspond to a level shown in the X-axis) in commercial Lu (wt %), distilled Lu (wt %), and distilled Lu (at %), respectively. Bluish columns indicate number of REMs (at %) in distilled Lu.

After the purification, the content of base metal increases from 99.15 to 99.955 wt %, in particular, at the expense of the decrease in the content of other REMs; the contents of more than forty impurities were 10^{-4}-10^{-5} at. % and the contents of eight impurities were 10^{-2} at. % each.

The alloys were studied in the as-cast and annealed states. The alloys were annealed at 500°C for 100 h. XRD studies were performed on a DRON-1.5 diffractometer using monochromatized (with a silicon (111) single crystal) Cu and Co K_α radiations; the measurements were performed at a step of 0.1 deg. A single crystal obtained was studied by Laue method using a RKB-86 chamber and Mo $K\alpha$ radiation. The powdered alloys were annealed in degasified quartz ampules. DTA of the Lu-Pd alloys was performed using a TAG-24 set up (SETARAM). Electron microscopic and electron microprobe studies were performed on a HITACHI S-800 electron microscope equipped with an INCA x-act energy dispersive X-ray microanalyzer.

3. RESULTS AND DISCUSSION

We studied cast alloys that were slowly cooled from the melt and powders of the alloys annealed at 1000°C for 100 h. All diffraction patterns of both cast and annealed powders show reflections beloning only to (depending on the composition) $LuPd_3$, Lu_3Pd_4, and LuPd. No reflections of $Lu_{10}Pd_{21}$ and Lu_2Pd_3 were found even after the annealing at 1000°C for 100 h. Figure 2 shows the X-ray diffraction pattern of the Pd-30 at.% Lu alloy. All fundamental reflections of $LuPd_3$ are clearly observed. According to phase diagrams of the other REM-Pd systems, in cast alloys, compounds that solidify from a single-phase melt (i.e. congruently) are formed. The $Lu_{10}Pd_{21}$ and Lu_2Pd_3 compounds are formed incongruently; namely, they are formed from the $A + L$ two-phase range, where A is a

previously formed intermetallic compound, i.e., $LuPd_3$ and Lu_3Pd_4. Upon cooling of these alloys, nonequilibrium phases arise quite easily. This is related to the low rate of the peritectic reaction between the *A* phase and the liquid. As such a nonequilibrium phase formed in the Lu-Pd alloys, the one with 30-45 at. % Lu and a hexagonal structure can be taken.

All of the X-ray diffraction patterns of the Pd-Lu alloys with 30-45 at. % show, along with the reflections of intermetallic compounds, a system of additional reflections that belong to non of the known compounds existing in the system. In Fig. 2, these reflections are marked by white circles. The structure of the phase was identified to be hexagonal with a *c/a* of from 0.45 to 0.52. The lattice parameters of the hexagonal phase vary depending on the alloy composition and annealing conditions. For the composition Pd-45.7 at. % Lu, the lattice parameters are *a* = 12.44 and *c* = 5.70 Å (for the as-cast state) and *a* = 13.42 and *c* = 6.43 Å (for the annealed state). This fact points to the variable composition of the phase and allows us to classify it as a bertholide compound [7]. Bertholides have no a strictly stoichiometic composition but are stable over a wide composition range, in contrast to dalthonides, which are characterized by a constant stoichiometric composition and constant lattice parameters. The bertholide phase indicates its nonequilibrium state since it is presented as a third phase in two-component alloys.

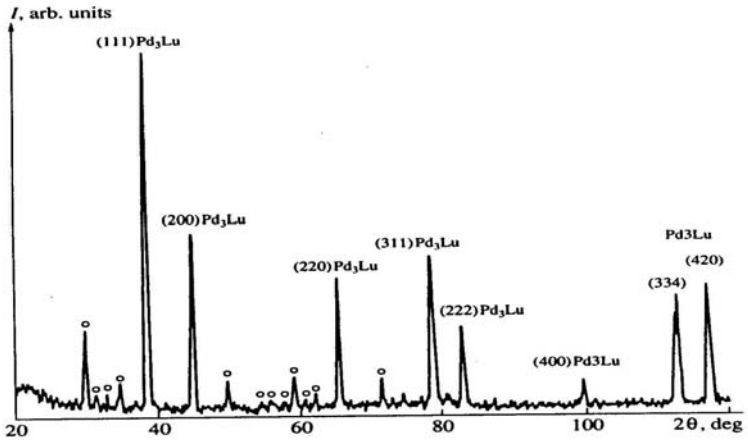

Fig. 2. X-ray diffraction pattern of the Pd-30 at. % Lu powder annealed at 1000°C for 100 h (Cu K_α radiation).

In order to realize the bertholide → dalthonide phase transformation, an additional annealing should be performed. Such an annealing at 500°C for 100 h was realized for the alloy with 44.5 at. % Lu, which results in the recrystallization and formation of 1-mm crystallites having different colores, namely golden, silvery, and dark. Golden and dark crystals were related to LuPd and $LuPd_3$. X-ray diffraction measurements performed for a silvery single crystal (Fig. 3) [8] showed that it has a monoclinic unit cell with the lattice parameters *a* = 7.78 Å, *b* = 8.90 Å, *c* = 12.21 Å, β = 117° and correspond to the Lu_2Pd_3 compound. The crystallographic data for the compounds of the Lu-Pd system in a range of from 0 to 50 at. % Lu are given in Tablle 1.

The $REM_{10}Pd_{21}$ compounds were identified for the systems with REM = Sm [9] and Tb [10]. The lattice parameters and interplanar spacings for the $Tb_{10}Pd_{21}$ compound were calculated and than identified in X-ray diffraction patterns. The formation of this compound in the Tb-Pd system takes place without the formation of bertholide phase. The possibility of the presence of the $Lu_{10}Pd_{21}$ compound was indicated by electron microprobe analysis of polished section of the annealed alloy with 32.5 at. % Lu (see Fig.

4). According to the microstructure of the alloy (nonequilibrium state), the formation of the phase by peritectic reaction may be assumed. The phases observed contain 31.5-32.5 at. % Lu ($Lu_{10}Pd_{21}$) (Fig. 4 b, spectra 1 and 2), 35.6-35.76 at. % Lu (eutectic) (Fig. 4a, spectrum 2, Fig. 4b, spectrum 3), and 28.1 at.% Lu ($LuPd_3$) (Fig. 4a, spectrum 1).

Boundaries of phase regions of the (Pd) and ($LuPd_3$) solid solutions at 1000°C were determined using X-ray diffraction data; they correspond to 10 and 21 at. % Lu, respectively. The eutectic point corresponds to 18 at. % Lu [4].

Table 1

Crystallographic data for the compounds of the Lu-Pd system

Phase	Lu, at. %	Space group	Structure type / Crystal lattice	*a*, Å	*b*, Å	*c*, Å	β, deg
$LuPd_3$	25	*Pm*3*m*	$AuCu_3$ Cubic	4.029	-	-	-
$Lu_{10}Pd_{21}$	32.3	*C*2/*m*	Monoclinic	24.85 [9] for $Sm_{10}Pd_{21}$ 24.74 [10] for $Tb_{10}Pd_{21}$	5.76 5.78	16.51 16.47	90.88 91.05
Lu_2Pd_3	40	*C*2/*m*	Monoclinic	7.78	8.90	12.21	117
Lu_3Pd_4	42.9	*R*-3	Pu_3Pd_4 Rhombohedral (in hexagonal setting)	12.87	5.64	-	-
LuPd	50	*Pm*-3*m*	CsCl Cubic	3.417	-	-	-

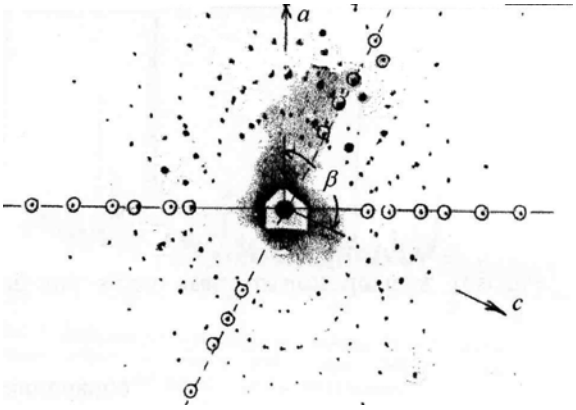

Fig. 3. Laue pattern of the single crystal obtained in the Pd-44.5 at. % alloy

Table 2 shows temperatures (according to DTA data) of invariant equilibria in the Lu-Pd system in a composition range of from 0 to 50 at. % Lu.

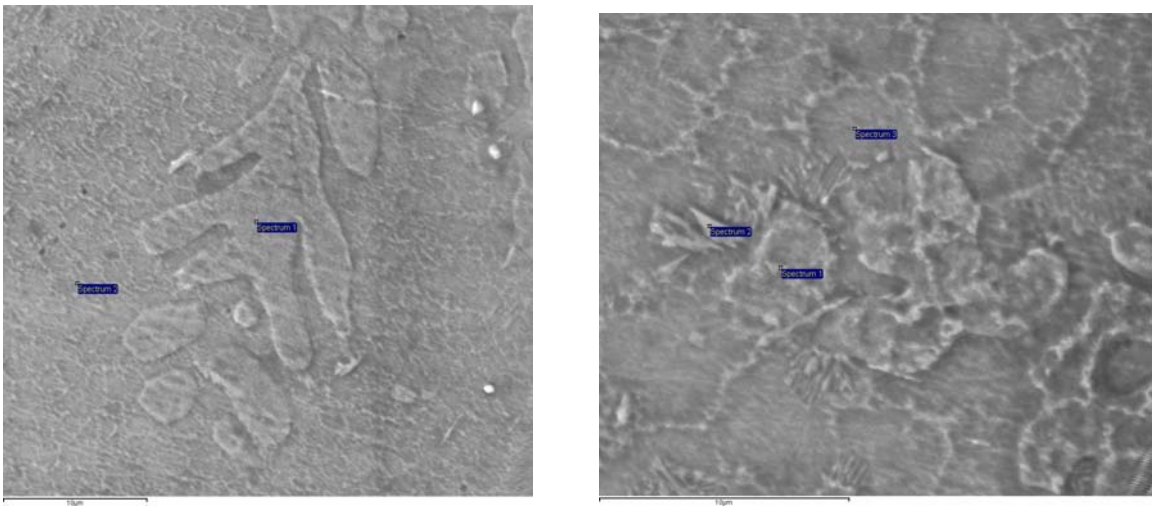

a b

Fig. 4. Electron micrographs of the as-cast Pd-32.5 at. % Lu alloy.

Table 2 Invariant equilibria in the Lu-Pd system

Reaction	T (°C)	Type	Phase	Composition (at.%)	
				Lu	Pd
L ⇔ $LuPd_3$	~1790	congruent	L, $LuPd_3$	25.0	75.0
L ⇔ LuPd	~1560	congruent	L, LuPd	50.0	50.0
L ⇔ Lu_3Pd_4	1480	congruent	L, Lu_3Pd_4	43.0	57.0
L ⇔ Lu_3Pd_4 + LuPd	1460	eutectic	L	45.0	54.0
			Lu_3Pd_4	43	57.0
			LuPd	50.0	50.0
L + ($LuPd_3$) ⇔ $Lu_{10}Pd_{21}$	~1410	peritectic	L	?	?
			($LuPd_3$)	28.0	72.0
			$Lu_{10}Pd_{21}$	32.5	67.5
L + Lu_3Pd_4 ⇔ Lu_2Pd_3	?1375	peritectic	L	?	?
			Lu_3Pd_4	43.0	57.0
			Lu_2Pd_3	40.0	60.0
L ⇔ $Lu_{10}Pd_{21}$ + Lu_2Pd_3	1360	eutectic	L	35.5	64.5
			$Lu_{10}Pd_{21}$	32.5	67.5
			Lu_2Pd_3	40.0	60.0
L ⇔ (Pd) + ($LuPd_3$)	1330	eutectic	L	18.0	82.0
			(Pd)	16.0	84.0
			($LuPd_3$)	21.0	79.0

A portion of the Lu-Pd phase diagram in a composition range of 0-50 at. % Lu is shown in Fig. 5.

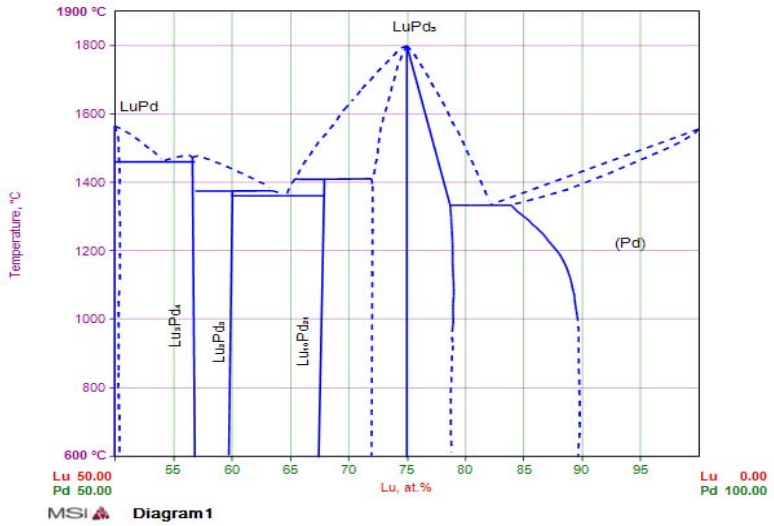

Fig. 5. Portion of the phase diagram of the Lu-Pd system.

CONCLUSIONS

The phase diagram of the Lu-Pd system is presented for a composition range of 0-50 at. % Lu. The formation of five intermetallic compounds is demonstrated. The formation of equilirbium phases in a range of 30-45 at. % Lu occurs through the formation of the nonequilibrium bertholide phase with a hexagonal structure.

REFERENCES

[1] GLADYSHEVSKII, E.I. and BODAK, O.I., *Crystalochemistry of rare-earth metal intermetallic compounds.* L'vov: Vysshaya shkola, 1982.

[2] MASSALSKI, T.B., (Ed.), *Binary alloy phase diagrams, 2nd edition,* Ohio: ASM International, Metals Park, 1990.

[3] LOEBICH, O.Y.R. and RAUB, E., Die Legierungen des Palladiums mit Yttrium, Samarium, Gadolinium, Dysprosium, Holmium und Erbium, *Less-common Met.*, 1973, v. 30, p. 47-62.

[4] BURKHANOV, G.S., ILYUSHIN, A.S., KOLCHUGINA, N.B., et al., Phase diagram of the Lu-Pd system in a range of 0-25 at. % Lu, *Izv. Ros. Akad. Nauk. Met.,* 1999, No. 6, p. 111-114.

[5] BURKHANOV, G.S., ROSHAN, N.R., KOLCHUGINA, N.B., et al., Palladium-rare-earth metals alloys – advanced materials for hydrogen power engineering, *Metallurgja,* 2008, No. 3, p. 248.

[6] GALOSHINA, E.V., KNYUZEV, Yu.V., KIRILLOVA, M.M., et al., Optica, electrical, and magnetic properties of Pd_3Lu and PdLu, *Fiz. Met. Metalloved.,* 1997, v. 84, No. 2, p. 59-66.

[7] KURNAKOV, N.S., *Vvedenie v fiziko-khimicheskii analiz*, Leningrad: ONTIKhIMTEORET, 1936.

[8] ILYUSHIN, A.S., KHATANOVA, N.A., RYKOVA, E.A., SILONOVA, E.V., Crystal structure parameters of the Lu_2Pd_3 intermetallic, *Vestn. Mosk. Univer., Ser. 3. Fiz. Astronom.,* 2001, No. 2, p. 47-51.

[9] FORNASINI, M.L., MUGNOLI, A., and PALENZONA, A., The crystal structure of $Sm_{10}Pd_{21}$, *Acta Crystallogr.,* 1979, v. B35, No. 9, p. 1950-1953.

[10] ILYUSHIN, A.S., KHATANOVA, N.A., BURKHANOV, G.S., et al., Formation of the Tb_3Pd_4 intermetallic in the Tb-Pd system, *Vestn. Mosk. Univer., Ser. 3. Fiz. Astronom.,* 2002, No. 5, p. 53-57.